Journal of Membrane Science 371 (2011) 37–44

Contents lists available at ScienceDirect

Journal of Membrane Science

journal homepage: www.elsevier.com/locate/memsci

Preparation of porous ion-exchange membranes (IEMs) and their characterizations

Chalida Klaysom[a], Seung-Hyeon Moon[b], Bradley P. Ladewig[a,c], G.Q. Max Lu[a,*], Lianzhou Wang[a,**]

[a] ARC Centre of Excellence for Functional Nanomaterials, School of Chemical Engineering and Australian Institute of Bioengineering and Nanotechnology, The University of Queensland, Qld 4072, Australia
[b] Gwangju Institute of Science and Technology, School of Environmental Science and Engineering, Gwangju 500-712, Republic of Korea
[c] Department of Chemical Engineering, Monash University, Vic 3800, Australia

ARTICLE INFO

Article history:
Received 28 October 2010
Received in revised form
24 December 2010
Accepted 9 January 2011
Available online 19 January 2011

Keywords:
Ion-exchange membranes
Two-step phase inversion
Porous structure
Electrodriving membranes
Desalination

ABSTRACT

Ion-exchange membranes consisting of sulfonated polyether sulfone with controllable porosities and structures were prepared via a two-step phase inversion procedure. The porosity of membranes has been deliberately controlled by adjusting drying conditions. It was experimentally evidenced that membranes with high porosities possessed excellent conductivity; they also had poor selectivity and mechanical stability, while non-porous membranes exhibited much better selectivity and mechanical strength at the cost of lower conductivity. Porous membranes with 2.11 mequiv cm^{-3} of fixed charged density, 0.33 mS cm^{-1} of conductivity, 0.9 of transport number and ~500 MPa of Young's modulus were obtained by carefully controlling the two-step phase inversion preparation process. The results from this work lead to better understanding of the relationship among the formation conditions in water/dimethylformamide (DMF)/sulfonated polyether sulfone (sPES) system, structures and properties of membranes, which may shed light on advanced membrane design for appropriate applications.

1. Introduction

High performance polymers with polyaryl skeletons such as polyarylsulfone, polyphenylsulfide and poly(ether ether)ketone have been widely studied as the alternative materials for perfluorosulfonic ionomers commercially known as Nafion in the past decades [1–4]. Aromatic skeleton not only makes the polymers thermally and mechanically stable, but also creates a variety of chemical modification opportunities such as simply electrophilic substitution. Among these high performance polymers, polyethersulfone (PES) has been considered as a good polymer matrix candidate for membrane formation due to its feasible processability and low cost. PES membranes have been modified and prepared via several techniques for applications as proton exchange membranes and nanofiltration membranes [1,4–16]. However, there were very limited works investigating the use of PES for membrane design especially porous IEMs suitable for various applications such as electrodialysis, desalination, gas separation process and water purification [8].

There are several important parameters required for an IEM which include conductivity, selectivity, thermal and mechanical stabilities, and chemical resistance when exposed to solutions under severe pH conditions. Unfortunately, to achieve one desirable property of IEMs is usually at the cost of another parameter. For instance, to make membranes high conductive, the membrane requires substantially amount of absorbed water to assist the ionic migration. While the high water uptake makes membranes mechanically unstable, and less selective. It is known that morphology of membranes has a great influence on their performance especially on the conductivity, selectivity and mechanical property. Therefore, it is crucially important to optimize the preparation steps carefully so that the prepared membranes may suit application with specific requirements. Unfortunately, there are still limited publications focusing on relationship among preparation conditions, membrane structures and their properties. In this work, we aim to study synthesis–structure–property rationale of the ion-exchange membranes. Polymer membranes based on sulfonated polyether sulfone (sPES) with various structures and pore sizes were synthesized via controlled phase inversion procedures, namely dry and wet phase inversion, or a combination of both methods. The properties of membrane including morphology, physical and electrochemical properties as well as their thermal and mechanical stabilities were investigated. The fraction of conducting region of each membrane was calculated using derived Sand's equation via chronopotentiometry technique. We were finally able to correlate the preparation conditions with membrane structures and properties to form a matrix for

* Corresponding author.
** Corresponding author. Tel.: +61 7 3365 4218; fax: +61 7 3365 4199.
E-mail addresses: maxlu@uq.edu.au (G.Q.M. Lu), l.wang@uq.edu.au (L. Wang).

0376-7388/$ – see front matter.
doi:10.1016/j.memsci.2011.01.008

selecting membranes suitable for the electrodriving membrane process.

2. Experimental

2.1. Materials

Polyethersulfone (RADEL A) provided by Solvay Advanced Polymers was dried at 120 °C for 24 h before use. The other chemicals were obtained commercially and were used as received without further purification.

2.2. Sulfonation

PES was sulfonated with chlorosulfonic acid. In a typical procedure, 20 g of PES was dissolved in 400 g of dichloromethane (Merk) under N_2 atmosphere with stirring at room temperature. Then, 20 cm^3 of chlorosulfonic acid (Sigma) was gradually and slowly added to the solution. The reaction was allowed to proceed for 150 min and then was terminated by precipitating the solution into cold water. The products were filtered and washed multiple times with deionized (DI) water until pH became approximately 5–6. Finally, the sulfonated PES products were dried at 120 °C for 2 days under vacuum. This sPES polymer was used as a polymer matrix for cation-exchange membranes.

2.3. Membrane preparation

In a typical preparation procedure for cation-exchange membranes, 3 g of sPES was first dissolved in 9 g of dimethylformamide (DMF) at 60 °C for 4 h under stirring. The polymer solution was then cast on glass substrates with different solution thickness using a doctor blade and then partially dried in a vacuum oven at 60 °C with different aging times from 0 to 48 h before precipitating in 60–70 °C DI water. The formed membrane sheet was peeled off and kept in DI water. The prepared membranes were treated in hot water for 2 h and then in 1 mol dm^{-3} HCl or 1 mol dm^{-3} NaCl for 24 h to obtain H^+ or Na^+ forms, respectively. After that, the membranes were rinsed with DI water and kept in DI water or 1 mol dm^{-3} NaCl solution. The prepared membranes were named by two numbers, representing their casting film thickness and the drying time in the dry phase inversion step. For instance, the membrane of 0.50 mm casting film thickness and 10 min of drying time was designated as 0.50–10. All the membranes were equilibrated in working solution for at least 6 h before used.

2.4. Membrane characterization

2.4.1. Membrane morphology

Morphology and structure of the membranes were observed using scanning electron microscopy (SEM) on a JEOL 6300 electron microscope. To obtain sharp cross-sectional surface fracture the samples were cut in liquid nitrogen, and then the captured water was dried out overnight in freeze dryer to preserve their structure.

2.4.2. Ion-exchange capacity (IEC) and water uptake of IEMs

IEC was measured using a titration method. The cation-exchange membrane was firstly soaked in 1 mol dm^{-3} HCl and then washed with DI water to remove excess HCl and was subsequently immersed into 1 mol dm^{-3} NaCl solution. The number of displaced protons from the membrane was determined by titration with 0.01 mol dm^{-3} standard NaOH solution using phenolphthalein as the indicator. Then the IEM was soaked in DI water for 24 h or more. After that, the membrane was taken out and water on the surface was wiped off with tissue paper. The wet weight of membrane was measured. Then the membrane was placed in an oven at 50 °C for 10 h or until there is no change in membrane weight. The dry weight of membrane was then recorded. The IEC and water uptake of membranes were calculated using Eqs. (1) and (2),

$$\text{IEC} = \frac{ab}{W_{dry}} \tag{1}$$

$$\text{Water uptake} = \frac{W_{wet} - W_{dry}}{W_{dry}} \tag{2}$$

where a is the concentration of NaOH solution used (mol dm^{-3}), b is the volume of NaOH solution used (dm^3), W_{dry} is the dry weight of the membrane and W_{wet} is the wet weight of the membrane.

2.4.3. Electrochemical properties of IEMs

2.4.3.1. Membrane resistance. An IEM was first equilibrated in 0.5 mol dm^{-3} NaCl before being placed in a two compartment cell between platinum electrodes with an effective area of 1 cm^2. The resistance of membranes was measured at room temperature by impedance spectroscopy (IS) using Solarton 225B in a frequency range from 1 to 10^6 Hz with an oscillating voltage of 100 mV amplitude [17]. The resistance corresponding to the phase angle closest to zero in the Bode diagram was recorded. Then, membrane resistance (R_{mem}) was calculated by subtraction of electrolyte resistance (here R_{sol} is the resistance of electrolyte in the cell measured without any membrane) from membrane resistance equilibrated in electrolyte solution (R_{cell}), according to the equation $R_{mem} = R_{cell} - R_{sol}$. Based on the electrical resistance measurement, the conductivity (σ, S cm^{-1}) of membranes was calculated according to Eq. (3),

$$\sigma = \frac{L}{R_{mem}A} \tag{3}$$

where R_{mem} was the resistance of membrane, L is the thickness of membrane (cm), and A is the effective area of the membrane (cm^2).

2.4.3.2. Membrane potential and transport number. Membrane potential was measured in a two compartment cell, in which a vertical membrane of 1.0 cm^2 effective area separated two solutions of 0.01 mol dm^{-3} NaCl and 0.05 mol dm^{-3} NaCl, respectively. The potential difference across the membrane was measured using a multimeter which was connected to Ag/AgCl reference electrodes. The transport number, $\bar{t}_+$, was calculated by the following equation:

$$E_m = \frac{RT}{F}(2\bar{t}_+ - 1)\ln\left(\frac{C_1}{C_2}\right) \tag{4}$$

where R is the gas constant, F is the Faraday constant, T is the absolute temperature, C_1 and C_2 are the concentration of electrolyte solutions in the testing cell.

2.4.3.3. Current–voltage characteristics and chronopotentiometry. The same two compartment cell was used to determine i–v curve and chronopotentiogram of the membrane in 0.025 mol dm^{-3} NaCl. The cell was connected to Solartron Multistat 1480 via two Pt electrodes. For i–v curve, the potential difference was applied across the membrane and the corresponding current was measured via two Ag/AgCl reference electrodes. The chronopotentiogram was conducted by applying constant current densities of 1–7.5 mA cm^{-2} and the corresponding potential was automatically recorded every 1 s for a period of 300 s.

2.4.4. Thermal and mechanical stabilities of membranes

Thermal stability of the membranes was investigated using thermogravimetric analysis (TGA) (Mettler Teledo) under nitrogen flow of 20 cm^3 min^{-1} at a heating rate of 10 °C min^{-1} in the range of 25–800 °C. The mechanical properties of membranes were measured by means of tensile test in wet state using an Instron 5800 at a speed of 2 mm min^{-1}. Membranes were cut into a rectangular

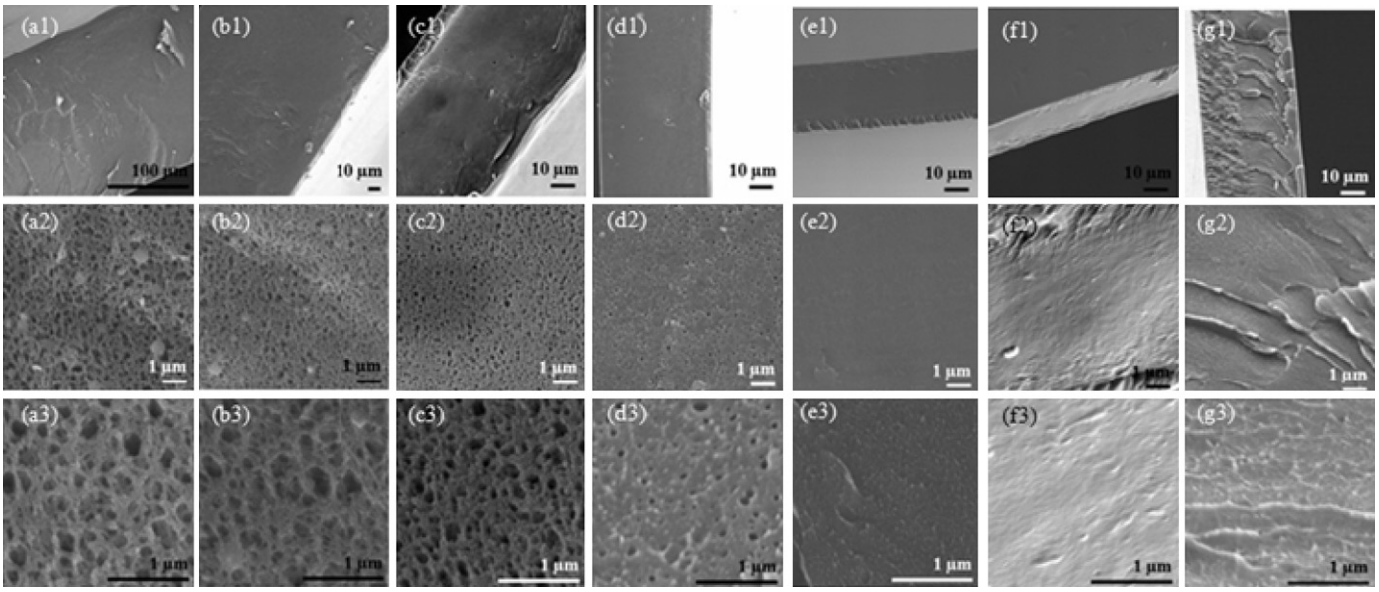

Fig. 1. SEM images of membranes prepared with different film thickness, and drying time; (a1–3) 0.45–0, (b1–3) 0.50–10, (c1–3) 0.45–5, (d1–3) 0.45–10, (e1–3) 0.45–15, (f1–3) 0.25–10, and (g1–3) 0.45–E. Note that E stands for solvent evaporation method from dying polymer film for 2 days.

shape with dimensions 50 mm × 5 mm. The gauge length of each specimen was 14 mm. At least five specimens from each sample were tested to acquire reliable average data.

3. Results and discussion

3.1. Preparation conditions and membrane structures

In this work sPES membranes with different porosities were synthesized using a so-called phase inversion process, namely wet phase inversion (precipitation), or dry phase inversion (solvent evaporation), or the combination of these two processes. In general, the morphologies of membrane depend highly on the preparation conditions. It has been reported that one of the key preparation parameters is the nonsolvent/solvent exchange rate, which can be controlled by tuning a number of synthesis conditions such as the concentration and viscosity of the casting solution, casting film thickness, additives and the temperatures of coagulation bath [11,18–20]. In our membrane formation process, DI water was used as the nonsolvent and the DMF was used as the solvent. The temperature of water coagulation bath was thermally controlled at 60–70 °C to reduce synthesis condition variation. Fig. 1 shows the morphologies of the prepared membranes. It was noticed that the obtained membranes showed macrovoid-free structure. The structure and porosity of the membranes can be easily controlled by controlling the wet film thickness and also film drying time before immersing in water bath to form membrane sheet.

As can be seen in Fig. 1, the membrane obtained from conventional precipitation method by immersing the nascent polymer film directly into water bath (it took casting solution around 1 min to form nascent film at room temperature, see Fig. 1a1–3) was highly porous with largest pore size compared to membranes prepared under other conditions. On the other hand, the membrane obtained from solvent evaporation method exhibited dense and non-porous structure (see Fig. 1g1–3). Typically for membranes prepared by phase inversion procedure, the properties of casting polymer solution have significant influence on the structure of the resultant membranes [16]. The more viscous the solution, the smaller exchange rate between nonsolvent and solvent in polymer film solution due to the rheological hindrance, thus resulting in membrane structure with smaller pore size. If we suddenly immersed the casted film in water bath, the low viscous polymer can be partly dissolved in water and membrane sheet could not be formed. In this work, to control the viscosity of the film solution and subsequently the nonsolvent/solvent exchange rate, the casting polymer film solution was further dried in the vacuum oven for longer period before it was precipitated in the water bath [11]. Most part of the solvent in casting film solution were removed when it was dried in the vacuum oven for longer than 15 min and completely evaporated after 2 days, leaving dense, nonporous structure in the resultant membranes. It has been reported that film thickness also plays a role in void formation and the asymmetric structure of the membranes [19,21,22]. In this work, the formation of the macrovoids could not be observed in all casting films with different thicknesses. However, the thinner the casting film is, the denser the membranes are because the solvent in the thinner film can be removed easier at the given drying time. In addition, it is well known that the structure of IEMs play crucial role on the performance of the membranes especially on their ionic conductivity and the selectivity. In general, membranes with larger pores or higher porosity possess better conductivity, however their selectivity are diminished. In the case of denser membranes, they possess better selectivity while suffer from high membrane resistance. More details about the effect of membrane structures on their electrochemical properties will be discussed in the next section.

3.2. Preparation condition–structure and properties relationship

The preparation condition and membrane properties were summarized in Table 1. It is worth noting that while the IEC of the prepared membrane was considerably constant under each condition, the water uptake was significantly increased with increasing the porosity of membranes. In addition, the conductivity of the membranes followed similar trend with the water uptake as continuous water channel enhances the mobility of ions. On the other hand, the fixed charge density of membranes increased with reduced pore size and porosity. It has been known that the selectivity of IEMs depends highly on the pore size and fixed charge density on the pore walls [23]. With higher porosity and larger pore size in the membrane, the Donnan exclusion become less effective and

Table 1
Formation conditions of IEMs and their properties.

Name	Drying time (min)	Casting thickness (mm)	Membrane thickness (mm)	Estimated pore diameter (nm)[a]	Water uptake (%)	IEC (mequiv g^{-1})	Fixed charge density (mequiv cm^{-3})	σ (mS cm^{-1})	$\bar{t}_i$
0.45–0	0	0.45	0.20 ± 0.01	100–200	274.96	0.74 ± 0.09	0.26	39.24	0.55
0.50–10	10	0.50	0.20 ± 0.01	100–200	265.38	0.70 ± 0.02	0.26	19.17	0.58
0.45–5	5	0.45	0.10 ± 0.01	50–100	238.71	0.67 ± 0.10	0.28	19.00	0.60
0.45–10	10	0.45	0.05 ± 0.01	>50	35.00	0.74 ± 0.02	2.11	0.331	0.90
0.45–15	15	0.45	0.03 ± 0.01	No visible pore	21.51	0.70 ± 0.01	3.18	0.083	0.95
0.25–10	10	0.25	0.01 ± 0.01	No visible pore	16.00	0.65 ± 0.10	4.06	0.034	0.95
0.45–E	2 days	0.45	0.03 ± 0.01	No visible pore	13.87	0.68 ± 0.02	4.85	0.072	0.95

[a] Estimated from SEM results.

thus the ionic species with any signs can freely move across [23]. As a consequence, the transport number, which is directly related to the selectivity of membranes, also increased with reduced pore sizes. In this case, the membrane with narrower pores and higher charge density will exclude co-ionic species and behave as the selective membrane.

3.3. Current–potential curves and chronopotentiogram

Once an IEM is placed in electrolyte solution under the applied potential difference, ionic species in the solution move into different directions according to the nature of their charges. Considering a cation-exchange membrane (CEM) system, cations move towards the cathode side by passing through CEM. The different migration rates of ions in IEM and in solution caused unavoidable phenomenon of concentration gradient near the interface between electrolyte solution and membranes. The counter-ions driven by electrostatic interaction of the charged functional groups will leave the depleting solution and accumulate near the surface on the other side of the membrane. The concentration gradient developed in the diffusion boundary layer near the membrane interface is different from that of adjacent bulk solution, known as the concentration polarization. It is important to investigate the transport phenomenon of the membrane particularly in the diffusion boundary layer to better understand the properties of IEMs for a given application. In this work, *i*–*v* curve and chronopotentiogram were used to investigate the electrochemical properties and transport phenomena of the prepared membranes. The limiting current density (LCD) is one of the crucial parameters of IEMs that normally limits the flux in the separation process especially in electrodriving process such as electrodialysis. The LCD of membranes can be determined from *i*–*v* curve, in which the inflection point between two regions of ohmic and plateau occurred [24].

A typical s-shape *i*–*v* curve was obtained from each of our prepared membranes (see Fig. 2), and the LCD was also listed in Table 2. The different slopes imply the differences in conductivity of each membrane. The membrane prepared from solvent evaporation method showed *i*–*v* characteristic with poorly defined plateau compared to the others. Typically, the shape of *i*–*v* curve depends on the testing conditions including the nature and surface properties

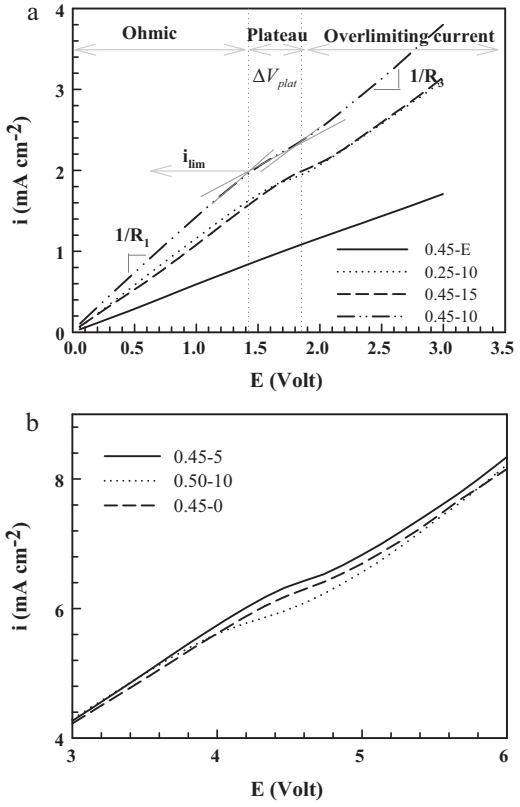

Fig. 2. (a and b) *i*–*v* curves of the prepared membranes tested in 0.025 M NaCl at room temperature.

of membranes, electrolyte solution, and the hydrodynamic condition in the testing system [25]. The results showed that the LCD increased following the trend of conductivity and water uptake. Based on the concentration polarization theory, the LCD can be expressed in the correlation among diffusion boundary layer thickness (δ), diffusion coefficient (D), and transport number as shown

Table 2
Characteristic values from chronopotentiograms of the prepared membranes.

Name/applied *i* (mA cm^{-2})	$\bar{t}_i$	LCD (mA cm^{-2})	τ[a]	τ[b]	ε
0.45–0/7.5	0.55	6.0	55.2	30.0	0.74
0.50–10/7.5	0.58	5.5	38.6	30.0	0.88
0.45–5/7.5	0.60	6.1	31.4	25.0	0.89
0.45–10/3.0	0.90	2.0	32.2	26.0	0.90
0.45–15/3.0	0.95	1.9	26.6	20.0	0.87
0.25–10/2.5	0.95	1.8	38.4	27.0	0.84
0.45–E/1.0	0.95	1.2	239.7	30.0	0.35

[a] Calculated value using Eq. (6).
[b] Value from chronopotentiogram.

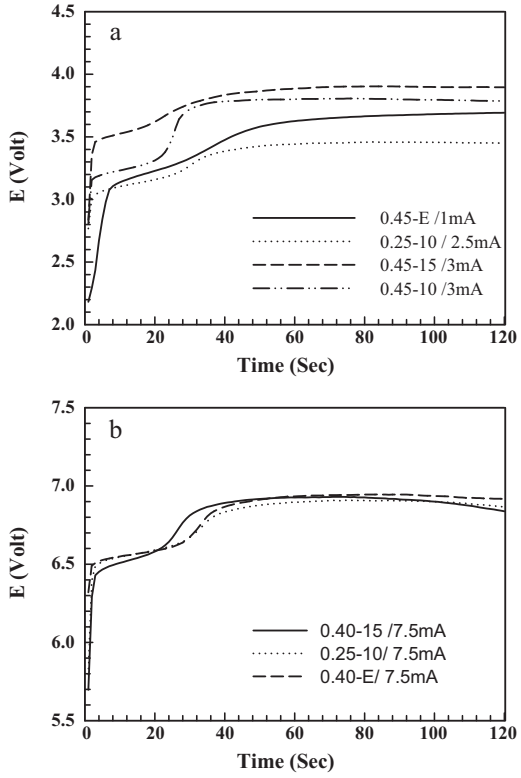

Fig. 3. (a and b) Chronopotentiogram of the prepared membranes in 0.025 M NaCl.

in Eq. (5);

$$i_{\lim} = \frac{|z|\,CFD}{\delta(\bar{t}_i - t_i)} \tag{5}$$

where i_{lim} is the limiting current density, C is the concentration of electrolyte, and z_i is the valence of the ith ion. The boundary layer thickness was considered to be the same for each membrane as it is well known as a function of hydrodynamic conditions such as feed flow or stirring rate, which was controlled in this study. Therefore, as expected, the LCD was proportional to the reciprocal of the transport number of the membranes.

Chronopotentiogram is well known as a powerful tool for studying the transport phenomena close to membrane surface [8,26–28]. This technique can also be used for investigating the concentration polarization near membrane interfaces and surface heterogeneity of the membranes by applying constant current density and measuring the potential difference during the course of testing. Fig. 3 shows the chronopotentiograms of the obtained membranes, which were measured at room temperature in diluted electrolyte solution.

Typical three stages in potential changes were obtained when constant current density was applied at higher LCD value. At the beginning a constant or slowly increased potential is observed due to the gradually developed concentration polarization. Then the potential shapely increased when the concentration of depleting solution near membrane–solution interface decreased to nearly zero before reaching steady stage at the end. The inflection point where significant potential change occurs, namely transition point and transition time, can be obtained from the chronopotentiogram. The curve shape and transition time depend highly on the morphology and the transport property of membranes. The transition time can be express in the well known Sand's equation;

$$\tau = \frac{(C_0 z_i F)^2 \pi D}{4i^2(\bar{t}_i - t_i)^2} \tag{6}$$

where i is the applied current density, C_0 is the concentration of electrolyte, and z_i is the valence of the ith ion. Characteristic values including the transition time from chronopotentiograms were summarized in Table 2.

Noting that the transition times calculated from Eq. (6) were higher than those derived from the chronopotentiograms. This implies that the membrane surface was not entirely conductive as assumed in the Sand's equation. The ion-exchange membranes might be considered inhomogeneous on the micro-scale containing conducting and non-conducting areas [8,29,30]. Because local current density near conducting area was higher than overall current density of the entire surface, less time was required for removing ionic species in the depleting solution, thus resulting in smaller transition time in the micro-heterogeneous membranes. In this work, the faction of conducting region, ε, was also calculated by derived Sand's equation as shown below:

$$\varepsilon = \frac{2i\pi^{1/2}(\bar{t}_i - t_i)}{C_o z_i F(\pi D)^{1/2}} \tag{7}$$

The fraction of conducting region increased to a peak with reduced porosity and then declined again when the membrane structure became too dense. Membrane prepared from two-steps phase inversion procedure with 10 min drying time and 0.45 mm film thickness possessed the highest fraction of the conducting region.

It is worth noting that these results revealed the membrane properties and behavior applicable in NaCl solution which is the major ion component of salt-rich water. However, in the system with divalent or other monovalent electrolytes, the membranes may react differently and provide different trends, because the electrochemical properties and transport behavior of the membranes also depend on the interaction between charge functional groups with ionic species. The different pore sizes have different sieving effects towards the transport of ionic species of different sizes. The influence of different electrolyte solutions on the membrane behaviors is needed to be further experimentally studied.

3.4. Thermal and mechanical stability of the membranes

It was clear that all the membranes exhibited very good thermal stability (Fig. 4a) and started to decompose at around 500 °C, which is sufficient for electrolydialysis operation. The mechanical stability of the prepared membranes was tested in wet condition at room temperature. Fig. 4c and d shows tensile stress, strain and Young's modulus of the prepared membranes. As we can see that the mechanical properties of the prepared membranes were significantly influenced by their structure and amount of water absorbed.

When tensile force was applied, IEMs with high porosity and high amount of water uptake can be largely extended because the absorbed water acts as the plasticizers and makes membrane flexible. However these membranes could not suffer from high pressure and thus resulted in low Young's modulus. On the other hand, membrane with denser structure possessed more robust structure and can stand to higher pressure with higher modulus properties. Membranes with moderate porosity or dense structure offered good mechanical stability, among which the membranes prepared from the solvent evaporation methods exhibited highest mechanical stability over 700 MPa the modulus. As the results, we can conclude that the membrane obtained from the conditions of 0.45 mm of casting thickness and 10 min of drying time with moderate porosity shows sufficient mechanical stability for the applications in desalination process.

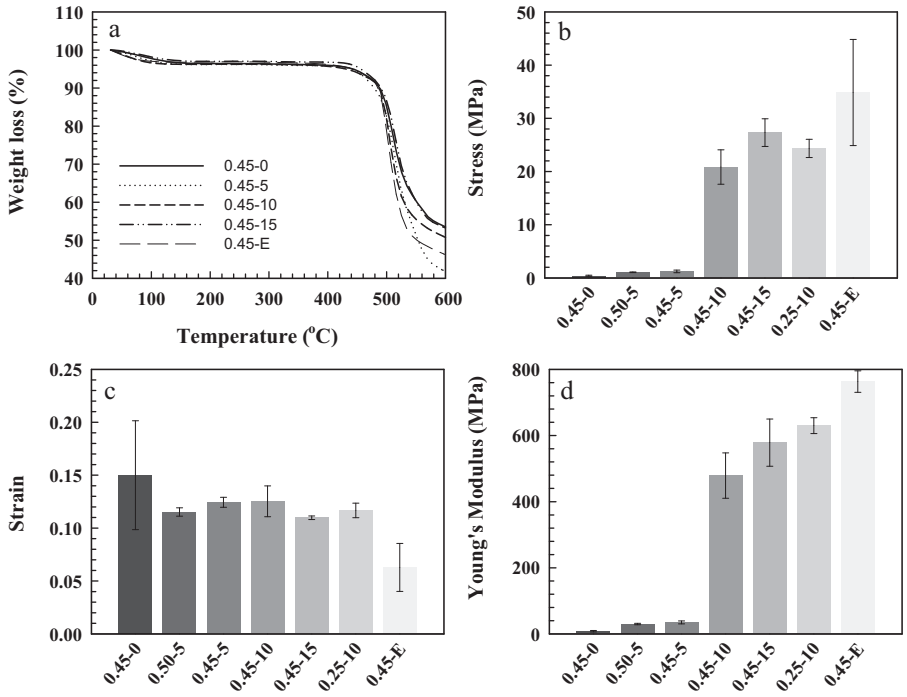

Fig. 4. Mechanical and thermal properties of the prepared membranes; (a) TGA curve, (b) tensile stress, (c) tensile stain, and (d) Young's modulus.

Preparation condition[a]	Drying time Viscosity		
Membrane structure	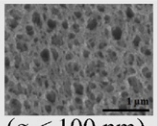 ($ø_p$< 100 nm)	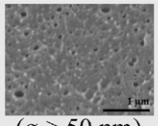 ($ø_p$> 50 nm)	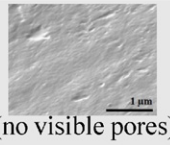 (no visible pores) Porosity Pore interconnection
Property	Water Uptake Conductivity Selectivity 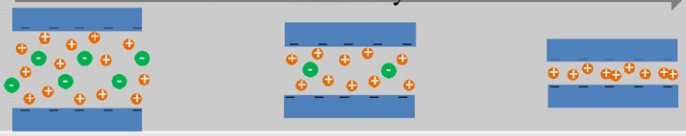		
Mechanical stability	Strength		
Recommended application	Microfiltration	Electrodriving process ED, PEMs, Ultrafiltration Desalination	PEMs, ED, RO Nanofiltration Gas separation process Desalination
Future improvement	Pore filling and modification	Surface modification Applied with higher DS polymer Composite with inorganic fillers or electrolyte polymer	

Note: [a]At the same casting film thickness and precipitation condition, → increase in parameter, ← decrease in parameter
ED, PEMs, RO are denoted for electrodialysis, proton-exchange membranes and reverse osmosis, respectively

Fig. 5. Correlation summary among preparation conditions, membrane structures and properties. *Note*: [a]At the same casting film thickness and precipitation conditions, → increase in parameter, ← decrease in parameter ED, PEMs, RO are denoted for electrodialysis, proton-exchange membranes and reverse osmosis, respectively.

3.5. Preparation conditions–structure–property relationship of IEMs

From the results in this work, we could correlate the preparation condition of ternary DMF/sPES/water system with membrane structure and property as summarized in Fig. 5.

By controlling drying time in dry phase inversion step before precipitating the casting polymer film in nonsolvent coagulation bath or controlling the viscosity of casting solution, porosity of the membrane can be easily controlled. As discussed in previous sections, the morphology of the membranes plays crucial role on the performance and mechanical property of the membranes. IEMs with pore interconnecting structure exhibited excellent conductivity, but poor mechanical strength. Though these membranes may not be suitable for membrane applications due to the insufficient mechanical stability, their high porosity creates potential for surface modification inside the pores [31,32]. For instance, with negative charge on the pores of membranes, pore-filling can be realized by filling other materials into the pores driven by of electrostatic force between the matrix membrane and the filling materials, which may offer specific surface properties for micro/ultrafiltration applications [32]. Therefore, surface modification of membrane pores is the promising tool to further tune this type of membranes. On the other hand, the dense IEMs possessed excellent selectivity and mechanical strength, but less ion conductivity. These membranes may be suitable for gas separation process, desalination by reverse osmosis (RO) or pervaporation desalination. With charged functional groups, they also showed a potential to use in ultra-filtration and microfiltration with repulsion of some ions to avoid fouling. Though their ion conductivity was not good compared to the porous ones, they are still promising for use as proton conducting membrane. In general, for a given IEM, its proton conductivity is much higher than its ionic conductivity. However, the detailed characterization for proton conducting membranes was required to confirm this prediction. We have applied this membrane as a proton conducting membrane in water splitting process for hydrogen production and published elsewhere [33]. Surprisingly, our prepared membranes performed as well as Nafion membrane in water splitting process. In addition, the ionic conductivity of the dense membranes can also be further improved by incorporating some functionalized inorganic fillers to provide extra functional groups and improve overall conductivity and selectivity while still maintain mechanical strength of the membranes [34]. On the other hand, higher degree of sulfonation with more fixed ionic functional groups on polymer main chains of PES is expected to provide higher ion conductivity in polymer matrix. It is our understanding that this correlation was specifically applied for membranes prepared from sPES in ternary DMF/sPES/water system, while it may also shed light on the preparation of other types of membranes. Note that in the present work we investigated mainly on the relationship among preparation conditions, structure and property of the membranes, whereas we are also clearly aware that the performance of the prepared membranes is a very important scope, which will be the subject of our future investigation.

4. Conclusions

The combination of dry and wet phase inversion was proved to be useful synthesis route for designing membranes with desired porosities and structures. The porosity of the membranes can be easily controlled by changing the drying period and casting film thickness. Increased drying period led to membranes with less porosity and denser structure. It was evidenced that the properties and performance of IEMs especially their conductivity and selectivity depended highly on membrane morphology and porosity. Though IEMs with interconnecting pore structure exhibited excellent ionic conductivity, their transport number and selectivity were proven to be very poor. On the other hand, membranes with smaller pores and denser texture were more selective, but less conductive. This is associated with the charged density of the membranes structure and pore surface. Membranes under optimized preparation conditions demonstrated 2.11 mequiv cm^{-3} of fixed charged density, 0.33 mS cm^{-1} of conductivity, 0.9 of transport number and ~500 MPa of modulus, which will satisfy the application requirements of electrodriving membranes. The findings of this study may lead to better understanding of the preparation conditions in ternary DMF/sPES/water system on the final structures of the membranes, which in turn affect their properties and electrochemical behavior.

Acknowledgements

The financial support from Australian Research Council (through its ARC Centre of Excellence and Discovery programs), CSIRO Advanced Membranes for Water Treatment Cluster Project, and Thai Government (through Higher Educational Strategic Scholarship for Frontier Research Network) is gratefully acknowledged. Additional thanks are due to Richard and Robin Webb for their useful discussion and helps on morphology characterization and sample preparation for SEM.

References

[1] S. Feng, Y. Shang, X. Xie, Y. Wang, J. Xu, Synthesis and characterization of crosslinked sulfonated poly(arylene ether sulfone) membranes for DMFC applications, J. Membr. Sci. 335 (2009) 13–20.
[2] C. Iojoiu, M. Marechal, F. Chabert, J.-Y. Sanchez, Mastering sulfonation of aromatic polysulfones: crucial for membranes for fuel cell application, Fuel Cells 5 (2005) 344–354.
[3] B.C. Johnson, I. Yilgor, C. Tran, M. Iqbal, J.P. Wightman, D.R. Lloyd, J.E. McGrath, Synthesis and characterization of sulfonated poly(arylene ether sulfones), J. Polym. Sci. Polym. Chem. Ed. 22 (1984) 721–737.
[4] M. Sankir, V.A. Bhanu, W.L. Harrison, H. Ghassemi, K.B. Wiles, T.E. Glass, A.E. Brink, M.H. Brink, J.E. McGrath, Synthesis and characterization of 3,3′-disulfonated-4,4′-dichlorodiphenyl sulfone (SDCDPS) monomer for proton exchange membranes (PEM) in fuel cell application, J. Appl. Polym. Sci. 100 (2006) 4595–4602.
[5] A. Bodalo, J.L. Gomez, E. Gomez, G. Leon, M. Tejera, Sulfonated polyethersulfone membranes in the desalination of aqueous solutions, Desalination 168 (2004) 277–282.
[6] H. Dai, R. Guan, C. Li, J. Liu, Development and characterization of sulfonated poly(ether sulfone) for proton exchange membrane materials, Solid State Ionics 178 (2007) 339–345.
[7] W.L. Harrison, Synthesis and Characterization of Sulfonated Poly(Arylene Ether Sulfone) Copolymers via Direct Copolymerization: Candidates for proton Exchange Membrane Fuel Cells, in Chemistry, Virginia Polytechnic Institute and State University, 2002.
[8] M.-S. Kang, Y.-J. Choi, I.-J. Choi, T.-H. Yoon, S.-H. Moon, Electrochemical characterization of sulfonated poly(arylene ether sulfone) (S-PES) cation-exchange membranes, J. Membr. Sci. 216 (2003) 39–53.
[9] I.C. Kim, J.G. Choi, T.M. Tak, Sulfonated polyethersulfone by heterogeneous method and its membrane performances, J. Appl. Polym. Sci. 74 (1999) 2046–2055.
[10] N.N. Krishnan, H.-J. Kim, M. Prasanna, E. Cho, E.-M. Shin, S.-Y. Lee, I.-H. Oh, S.-A. Hong, T.-H. Lim, Synthesis and characterization of sulfonated poly(ether sulfone) copolymer membranes for fuel cell applications, J. Power Sources 158 (2006) 1246–1250.
[11] C. Barth, M.C. Goncalves, A.T.N. Pires, J. Roeder, B.A. Wolf, Asymmetric polysulfone and polyethersulfone membranes: effects of thermodynamic conditions during formation on their performance, J. Membr. Sci. 169 (2000) 287–299.
[12] B. Smitha, S. Sridhar, A.A. Khan, Synthesis and characterization of proton conducting polymer membranes for fuel cells, J. Membr. Sci. 225 (2003) 63–76.
[13] F. Wang, M. Hickner, Y.S. Kim, T.Z. Zawodzinski, J.E. McGrath, Direct polymerization of sulfonated poly(arylene ether sulfone) random (statistical) copolymers: candidates for new proton exchange membranes, J. Membr. Sci. 197 (2002) 231–242.
[14] J.F. Blanco, Q.T. Nguyen, P. Schaetzel, Novel hydropilic membrane materials: sulfonated polyethersulfone Cardo, J. Membr. Sci. 186 (2001) 267–279.
[15] J.F. Blanco, Q.T. Nguyen, P. Schaetzel, Sulfonation of polysulfones: suitability of the sulfonated materials for asymmetric membrane preparation, J. Appl. Polym. Sci. 84 (2002) 2461–2473.

[16] M. Wang, L.-G. Wu, J.-X. Mo, C.-J. Gao, The preparation and characterization of novel charged polyacrylonitrile/PES-C blend membranes used for ultrafiltration, J. Membr. Sci. 274 (2006) 200–208.
[17] R.K. Nagarale, G.S. Gohil, V.K. Shahi, Recent developments on ion-exchange membranes and electro-membrane processes, Adv. Colloid Interface Sci. 119 (2006) 97–130.
[18] J. Barzin, B. Sadatnia, Theoretical phase diagram calculation and membrane morphology evaluation for water/solvent/polyethersulfone system, Polymer 48 (2007) 1620–1631.
[19] A. Conesa, T. Gumi, C. Palet, Membrane thickness and preparation temperature as key parameters for controlling the macrovoid structure of chiral activated membranes (CAM), J. Membr. Sci. 287 (2007) 29–40.
[20] P. Van de Witte, P.J. Dijkstra, J.W.A. Van de Berg, J. Feijen, Phase separation processes in polymer solutions in relation to membrane formation, J. Membr. Sci. 117 (1996) 1–31.
[21] Y. Termonia, Fundamentals of polymer coagulation, J. Polym. Sci. Part B: Polym. Phys. 33 (1995) 279–288.
[22] B.F. Barton, J.L. Reeve, M. A.J., Observations on the dynamics of nonsolvent-induced phase inversion, J. Polym. Sci. Part B: Polym. Phys. 35 (1997) 569–585.
[23] K. Sollner, An outline of the basic electrochemistry of porous membranes, J. Dental Res. 53 (1974) 267–279.
[24] J. Balster, O. Krupenko, I. Punt, D.F. Stamatialis, M. Wessling, Preparation and characterisation of monovalent ion selective cation exchange membranes based on sulphonated poly(ether ether ketone), J. Membr. Sci. 263 (2005) 137–145.
[25] V.M. Aguilella, S. Mafe, J.A. Manzanares, J. Pellicer, Current–voltage curves for ion-exchange membranes. Contributions to the total potential drop, J. Membr. Sci. 61 (1991) 177–190.
[26] H.-J. Lee, M.-K. Hong, S.-D. Han, S.-H. Moon, Influence of the heterogeneous structure on the electrochemical properties of anion exchange membranes, J. Membr. Sci. 320 (2008) 549–555.
[27] N. Pismenskaya, P. Sistat, P. Huguet, V. Nikonenko, G. Pourcelly, Chronopotentiometry applied to the study of ion transfer through anion exchange membranes, J. Membr. Sci. 228 (2004) 65–76.
[28] F.G. Wilhelm, N.F.A. Van der Vegt, M. Wessling, H. Strathmann, Chronopotentiometry for the advanced current–voltage characterisation of bipolar membranes, J. Electroanal. Chem. (2001) 152–166.
[29] J.-H. Choi, S.-H. Moon, Pore size characterization of cation-exchange membranes by chronopotentiometry using homologous amine ions, J. Membr. Sci. 191 (2001) 225–236.
[30] J.-H. Choi, S.-H. Kim, S.-H. Moon, Heterogeneity of ion-exchange membranes: the effects of membrane heterogeneity on transport properties, Adv. Colloid Interface Sci. 241 (2001) 120–126.
[31] S. Moghaddam, E. Pengwang, Y.-B. Jiang, A.R. Garcia, D.J. Burnett, C.J. Brinker, R.I. Masel, M.A. Shannon, An inorganic–organic proton exchange membrane for fuel cells with a controlled nanoscale pore structure, Nat. Nanotechnol. 5 (2010) 230–236.
[32] W. Jiang, R.F. Childs, A.M. Mika, J.M. Dickson, Pore-filled membranes capable of selective negative rejections, Nat. Sci. 1 (2003) 21–26.
[33] R. Marschall, C. Klaysom, A. Mukherji, G.Q.M. Lu, L.Wang, Composite polymer membranes for clean hydrogen production via sunlight-driven photoelectrochemical water splitting process, ChemSusChem, submitted for publication.
[34] C. Klaysom, R. Marschall, B.P. Ladewig, G.Q.M. Lu, L. Wang, Synthesis of composite ion-exchange membranes and their electrochemical properties for desalination applications, J. Mater. Chem. 20 (2010) 4669–4674.